Dynamics of random dipoles: chaos versus ferromagnetism

F Borgonovi[1,2] and G L Celardo[1]

[1] Dipartimento di Matematica e Fisica, Università Cattolica, via Musei 41, I-25121 Brescia, Italy
[2] INFN, Sezione di Pavia, Via Bassi 6, I-27100 Pavia, Italy
E-mail: fausto.borgonovi@unicatt.it and nicedirac@gmail.com (G L Celardo)

Abstract. The microcanonical dynamics of an ensemble of random magnetic dipoles in a needle has been investigated. Due to the presence of a constant of motion in the 1D case, a 'dimensional' phase transition in the quasi-one-dimensional case has been found separating a paramagnetic chaotic phase from a ferromagnetic regular one. In particular, a simple criterion for the transition has been formulated and an intensive critical parameter found. Numerical simulations support our understanding of this complex phenomenon.

Keywords: disordered systems (theory), ergodicity breaking (theory), dynamical processes (theory)

Contents

1. Introduction

A truly comprehensive understanding of magnetism at the nanoscale is still lacking and has important consequences in the technology of memory and information processing devices.

Many unsolved problems about the magnetic properties of diluted spin systems have recently attracted a great deal of attention. Among the open problems there is the emergence of ferromagnetism in doped diluted systems [1], where the Curie temperatures can be as high as 300 K, and a deep theoretical understanding of the magnetic properties of dilute dipole systems (spin glass transition, ferromagnetic and antiferromagnetic transitions).

Here we will concentrate on randomly arranged dilute classical dipoles, which are called dipole glasses. Many results in the literature, sometimes controversial, exist on such kinds of systems. Magnetic properties of dipole–dipole interacting spins are particularly difficult to study due to many factors: the long range nature of the interaction, anisotropy and frustration. Long range and anisotropy can induce ergodicity breaking [2] in a system. Breaking of ergodicity, a concept introduced by Palmer [2], and recently found explicitly [3, 4] in a class of long-ranged anisotropic spin systems, is a key word in understanding phase transitions too, even if it should not be confused with breaking of symmetry [5]. Speaking loosely, a few constants of motion, such as the energy or the angular momentum in a particular geometry, produce a separation of the allowable phase space into two or more subspaces over which the motion is constrained. In [3] the energy at which the separation occurs has been calculated explicitly for an anisotropic 1D classical Heisenberg system. In that case both the anisotropy and the long-ranged nature [6] of the inter-spin interaction, are essential ingredients in order to have breaking of ergodicity [7]. On the other hand, frustration, that is the impossibility to attain a global minimal energy minimizing locally the interactions, induces a dependence of the ferromagnetic and antiferromagnetic properties on the lattice geometry [8].

Other results concerning the so-called Ising dipole glass can also be found in the literature, where Ising simply means uni-axial. To quote but a few: a spin glass transition

for high concentration, using Monte Carlo simulation [9, 10], mean-field spin glass transition at low concentration depending on the lattice geometry [11], absence of spin glass transition for low concentration using Wang–Landau Monte Carlo simulations [12] or the recent spin glass transition at non-zero temperature from extensive numerical simulation [13].

In this paper we will focus our analysis on a dipole glass of freely rotating classical dipoles. First of all, the dipole glass is a typical example of a very frustrated system [14]–[16], so that different ground state configurations can exist, depending on the geometry and the spin concentration. Results in the canonical ensemble typically consider a mean-field approach, and it is common lore that the random positions of the dipoles induce magnetic field fluctuations. These fluctuations do not vanish at $T \to 0$, unlike thermal fluctuations, and tend to suppress magnetic order even at $T = 0$ [15, 16]. So, magnetic order is expected to happen only for high impurity concentrations (and low temperatures) [16]–[18]. Mean-field theories consider only the equilibrium properties and do not take into account the time needed to reach the equilibrium situation and finite size effects. On the other hand, the question of how long a metastable state can last is a major issue in determining the magnetic properties of a system.

In this paper we study the microcanonical dynamics, reserving the study of the influence of a thermal bath for further investigations. We analyze the microcanonical dynamics of dipoles put at the vertices of a cubic lattice (so that their relative distance cannot be smaller than the lattice size), only on the basis of the Landau–Lifshitz–Gilbert equations of motion. 3D dipole–dipole interacting systems can be realized quite easily in the laboratory, for instance doping a non-magnetic media with paramagnetic ions, weakly interacting with the lattice and with a relative inter-dipole distance sufficiently large in order to neglect the Heisenberg interaction (and therefore with a low concentration). The choice of studying a random glass instead of a system composed of dipoles regularly arranged in some lattice is twofold: on the one hand, it is relatively easy to dope a system putting some paramagnetic doping ions in a random way inside any non-magnetic media. On the other hand, a 3D cubic lattice with a full concentration of dopant ions $\delta = 1$, even if extremely thin, does not have a ferromagnetic ground state [19], so that another type of transition should be considered (paramagnetic/antiferromagnetic).

Anticipating some of the results, we have found that, taking into account a typical experimental situation with needle-shaped sample, at low dipole concentration a further constant of motion appears that induces a kind of 'phase' transition related to invariant tori, which separate the allowable phase into many disconnected regions. This result seems to indicate that, at very low concentration a system of random dipoles in a needle resemble a one-dimensional arrangement of dipoles, and thus can have ferromagnetic behavior. In this particular case, the ergodicity breaking is not due to an increase of energy, but to an increase of perturbation, which means the tendency to a transformation from a needle shape (quasi-1D system) to a cubic shape (3D shape). In a sense, these results are more akin to the standard perturbation theory in classical dynamical systems [20, 21], re-interpreted in the light of phase transitions induced by demagnetization times [22].

In the future we are going to study the same system in contact with a thermal bath. In this case the presence of the ergodicity breaking found in [3, 4] should influence the demagnetization times. In the microcanonical case, the presence of this ergodicity breaking is hidden by the quasi-integrability of motion.
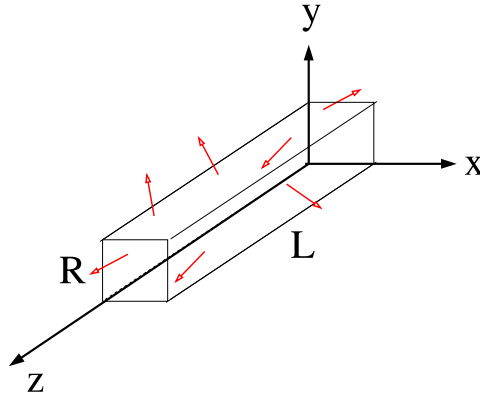
Figure 1. Needle geometry. The classical dipoles are put in a random way on the vertices of a cubic lattice of size a. R and L are given in units of the lattice size a.

2. The classical model and the perturbative approach

Let us consider a system of N classical dipoles $\vec{\mu}_i$ randomly put at the nodes of a 3D gridded box $R \times R \times L$, with $L \gg R$, and low concentration $\delta \ll 1$, as indicated in figure 1.

From the physical point of view it represents a dilute system of paramagnetic ions in a non-magnetic bulk, with a concentration $\delta = N/N_s$, where $N_s = R^2 L$ is the number of allowable sites in the 3D lattice. As explained above, such a system can be realized in the laboratory, doping a non-magnetic system having a cubic lattice with paramagnetic impurities. In the last decade, a lot of experimental and theoretical results have been collected for doped TiO_2 and others [1]. If the dipoles weakly interact with the lattice and if their average distance is much greater than the Bohr radius, we can simply neglect the Heisenberg (exchange) interaction and represent their mutual interaction and dynamics with a pure dipole–dipole interaction energy:

$$E = \frac{\mu_0 \mu^2}{4\pi a^3} \sum_{i=1}^{N} \sum_{j>i} \frac{1}{|r_{ij}|^3}[\vec{S}_i \cdot \vec{S}_j - 3(\vec{S}_i \cdot \hat{r}_{ij})(\vec{S}_j \cdot \hat{r}_{ij})]. \tag{1}$$

Here $\vec{S}_i$ is the ith dimensionless spin vector:

$$\vec{S}_i \cdot \vec{S}_i = 1, \tag{2}$$

μ is the magnetic moment of the paramagnetic doping ions and r_{ij} is the distance between the ith and the jth spin in units of the lattice spacing a.

The dynamics is described by the Landau–Lifshitz–Gilbert equations of motion:

$$\frac{\mathrm{d}}{\mathrm{d}t}\vec{\mu}_k = \gamma \vec{\mu}_k \times \frac{\delta E}{\delta \vec{\mu}_k}, \tag{3}$$

where $\vec{\mu}_k = \mu \vec{S}_k$ and γ is the gyromagnetic ratio.

They can be rewritten in the dimensionless form:

$$\frac{\mathrm{d}}{\mathrm{d}\tau}\vec{S}_k = \vec{S}_k \times \frac{\delta E_0}{\delta \vec{S}_k}, \tag{4}$$

where the following dimensionless quantities have been introduced:

$$E_0 = E\frac{4\pi a^3}{\mu_0 \mu^2} \qquad \tau = \omega t, \qquad \text{with } \omega = \frac{\gamma \mu \mu_0}{4\pi a^3}. \tag{5}$$

The system of equations considered above conserves the energy (1) and the squared moduli of the spins (2).

The diluted doped quasi-1D system can be magnetized with a strong magnetic field directed along L, the longest axis (z axis). The questions we would like to answer is the following: what is the dependence of the average demagnetization time and its fluctuations on the system parameters?

The relevant parameters to take into account are the concentration δ of paramagnetic ions and the aspect ratio $\epsilon = R/L$. In principle, due to the long-ranged nature of the dipole interaction, one could ask whether there are effects dependent on both the system size and the number of doping spins N, even if, in quasi-1D systems, the dipole interaction can be treated as a short range interaction.

From the point of view of the equations of motion (4), if the N dipoles are lying along a straight line ($R = 0 \Rightarrow \epsilon = 0$), there is a further constant of motion, i.e. $M_z = (1/N)\sum_k S_k^z$. Therefore, for a 1D system, the answer to the first question above is very simple: a state with any initial magnetization $M_z(0) \neq 0$ will keep the initial magnetization forever. The natural question thus becomes: what happens for $\epsilon \neq 0$? Will a magnetized state demagnetize and how much time does it take to do that?

The classical dynamical picture can be simplified by adopting a perturbative approach, namely approximating the unit vector between two spins as follows:

$$\hat{r}_{ij} = \cos\theta_{ij}\hat{z} + \sin\theta_{ij}(\cos\phi_{ij}\hat{x} + \sin\phi_{ij}\hat{y}) \simeq \hat{z} + (\epsilon N)(\cos\phi_{ij}\hat{x} + \sin\phi_{ij}\hat{y}) \tag{6}$$

where $\hat{x}, \hat{y}, \hat{z}$ are the unit vectors, ϕ_{ij} are the azimuthal angles with respect the z axis and $\theta_{i,j}$ are the polar angles. In the last equation we approximate $\cos\theta_{ij} \simeq 1$ and $\sin\theta_{i,j} \simeq R/\langle d\rangle$, where, for dilute dipoles in a needle geometry, $\langle d\rangle = L/N$ is the average distance among spins. The energy (1), to first order in ϵN, becomes $E_0 = H_0 + \epsilon N V$, where H_0 is the energy part that conserve M_z, and V is the perturbation:

$$\begin{aligned} H_0 &= \frac{1}{2}\sum_{i=1}^{N}\sum_{j\neq i}\frac{1}{|r_{ij}|^3}[S_i^x S_j^x + S_i^y S_j^y - 2S_i^z S_j^z], \\ V &= -3\sum_{i=1}^{N}\sum_{j\neq i}\frac{1}{|r_{ij}|^3}[\cos\phi_{ij}S_i^z S_j^x + \sin\phi_{ij}S_i^z S_j^y]. \end{aligned} \tag{7}$$

The equations of motion for the macroscopic variables, $M_{x,y,z}$, can be written as

$$\frac{\mathrm{d}M_z}{\mathrm{d}\tau} = 3\epsilon \sum_k \sum_{i\neq k}\frac{1}{|r_{ik}|^3}S_i^z(S_k^y\cos\phi_{ik} - S_k^x\sin\phi_{ik})$$

$$\frac{\mathrm{d}M_y}{\mathrm{d}\tau} = \frac{3}{N}\sum_k \sum_{i\neq k}\frac{1}{|r_{ik}|^3}\{S_i^z S_k^x + \epsilon N[S_k^x S_i^y\sin\phi_{ik} + (S_k^x S_i^x - S_k^z S_i^z)\cos\phi_{ik}]\} \tag{8}$$

$$\frac{\mathrm{d}M_x}{\mathrm{d}\tau} = -\frac{3}{N}\sum_k \sum_{i\neq k}\frac{1}{|r_{ik}|^3}\{S_i^z S_k^y + \epsilon N[S_k^x S_i^y\cos\phi_{ik} + (S_k^y S_i^y - S_k^z S_i^z)\sin\phi_{ik}]\},$$
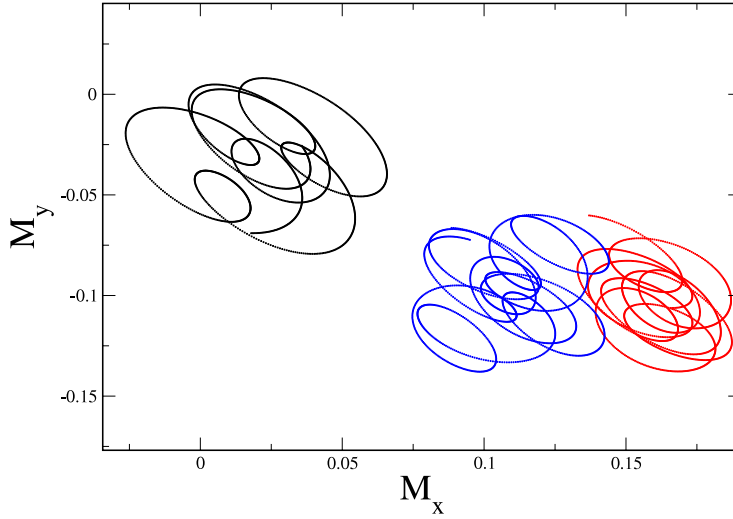
Figure 2. Three different trajectories, for $R = 4$, $L = 4000$, $\delta = 10^{-3}$, $N = 64$, in the integrable case. Initially spins are chosen with random components on the unit sphere.

and, in particular, for $\epsilon = 0$ we have

$$\frac{\mathrm{d}M_z}{\mathrm{d}\tau} = 0 \qquad \frac{\mathrm{d}M_y}{\mathrm{d}\tau} = \frac{1}{N}\sum_k \omega_k S_k^x \qquad \frac{\mathrm{d}M_x}{\mathrm{d}\tau} = -\frac{1}{N}\sum_k \omega_k S_k^y, \qquad (9)$$

having defined, the average 'local' frequencies:

$$\omega_k = 3\sum_{i\neq k} \frac{1}{|r_{ik}|^3} S_i^z. \qquad (10)$$

These equations describe a kind of rotation in the plane perpendicular to the z magnetization (which is a constant of motion). Therefore one could expect that for $\epsilon N \ll 1$ a rotational-like motion about the z axis persists, while M_z remains a quasi-constant of motion. This is what can be observed, for instance, by a direct inspection of the trajectories of the macroscopic vector $\vec{M}$, in the plane x, y, see figure 2, where few selected trajectories have been iterated in time, for $\epsilon = 10^{-3}$ and $N = 64$. Quite naturally, on increasing the perturbation strength ϵ, one could expect that the invariant tori $M_z = $ const will be broken and, eventually, a stochastic motion of the macroscopic variable M_z will appear. In section 3 we will study the survival of invariant tori under the dimensional perturbation $\epsilon N > 0$.

3. The chaotic–paramagnetic and the integrable-ferromagnetic phases

The dynamical behavior of the system can be characterized by a 'regular region' $\epsilon N < 1$ in which the magnetization $M_z(\tau)$ is bounded in a small interval δM_z, while, for $\epsilon N > 1$, $M_z(\tau)$ quickly decays to zero. To be more precise, the transition across $(\epsilon N)_{\mathrm{cr}} = 1$ is smooth, namely there is a region of ϵN values in which the initial magnetization decays to some non-zero constant when the time τ becomes large.
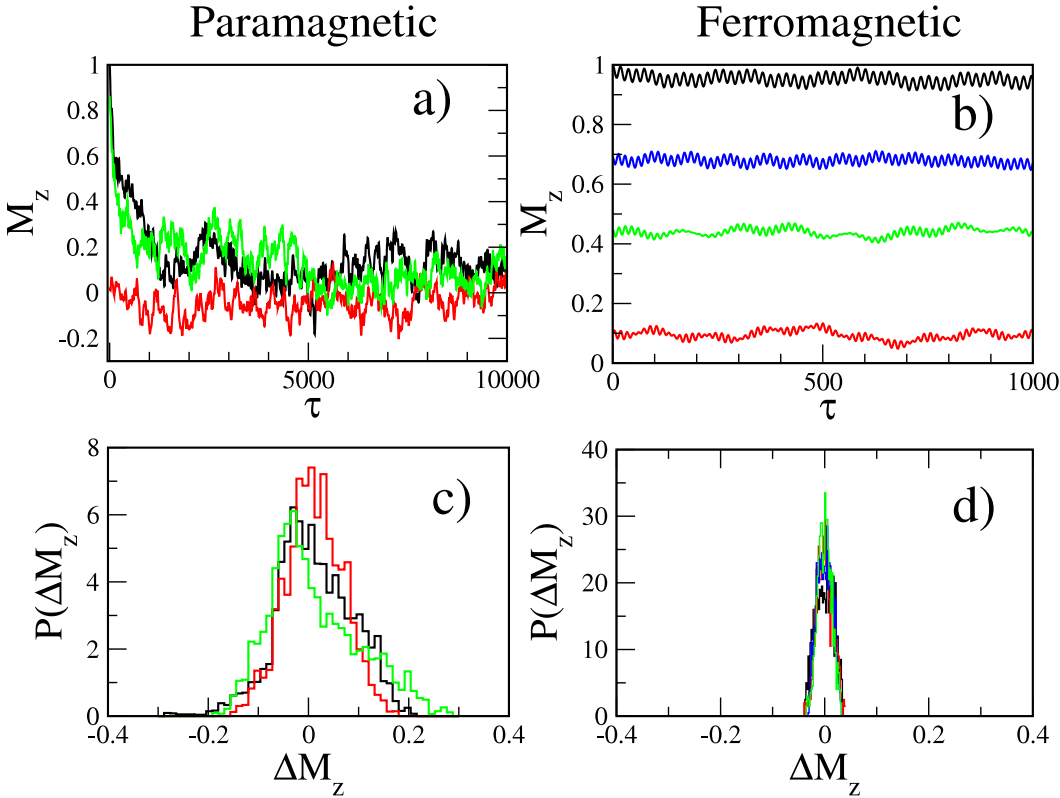
Paramagnetic   Ferromagnetic

Figure 3. Data in this figure refer to systems with $N = 64$ spins and a concentration $\delta = 10^{-3}$. The time behavior of the magnetization is shown, for different initial conditions, in the overcritical case $\epsilon = 0.125$ (a) ($L = 160, R = 20$) and in the undercritical case $\epsilon = 10^{-3}$ (b) ($L = 4000, R = 4$). In (c) and (d) the probability distribution functions for the fluctuations $\Delta M_z = (\langle M_z^2 \rangle - \langle M_z \rangle^2)^{1/2}$ around the equilibrium value are shown for the data given respectively in (a) and (b).

The critical value of the perturbation strength $(\epsilon N)_{\mathrm{cr}} = 1$ can be obtained with the following hand-waving argument. Let us divide the 3D box into $n = L/R = 1/\epsilon$ small cubic boxes of side R. If the impurities concentration δ is sufficiently small in order to have only one spin inside each R-sided box then the system is approximately one-dimensional and M_z can be considered an approximate constant of motion. Otherwise, for large δ, the system behaves like a 3D system and M_z can spread everywhere. In other words, in order to have less than one spin in each R^3 block one should have $N/n < 1$, or $\epsilon N < (\epsilon N)_{\mathrm{cr}} = 1$.

Moreover the study of the dynamics done in section 2 suggests we take as a small parameter ϵN and to look for ferromagnetism when $\epsilon N < 1$. Note that this choice is also appropriate from the thermodynamic point of view since $\epsilon N = RN/L$ is an intensive parameters in the large N limit $L \to \infty$, $N \to \infty$, $N/L = $ const, with R fixed.

An example is shown in figure 3, where the dynamics of magnetization has been plotted in the overcritical case ($\epsilon N > 1$, figure 3(a)) and in the undercritical one ($\epsilon N < 1$, figure 3(b)). Different trajectories, corresponding to different initial conditions $M_z(0)$, have been shown in different colors. As one can see, in the 'paramagnetic' phase ($\epsilon N > 1$) the magnetization first decays to zero and then it fluctuates randomly around zero. In
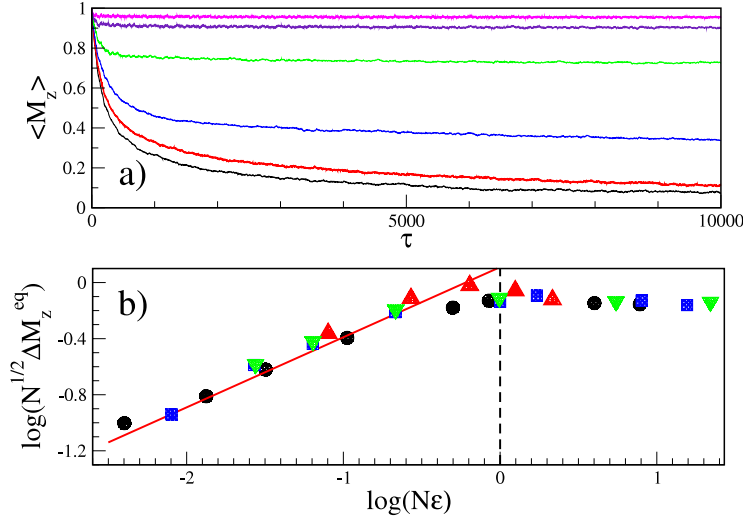
Figure 4. (a) Time behavior of the average magnetization for different values of the aspect ratio $\epsilon = 1.25 \times 10^{-4}, 2.9 \times 10^{-4}, 9.8 \times 10^{-4}, 4.5 \times 10^{-3}, 2.5 \times 10^{-2}, 10^{-1}$ (from the upper to the lower), fixed number of spins $N = 220$ and fixed concentration $\delta = 10^{-3}$. The average is taken over 100 different random configurations. Initially we choose $S_i^z(0) = 1$, $i = 1, \ldots, N$. (b) Dependence of the equilibrium value of fluctuations as a function of ϵN. Dashed vertical line indicates the critical value $\epsilon N = 1$. Red line indicates the dependence $\sqrt{N\epsilon}$. Different symbols stand for: $N = 40, \delta = 5 \times 10^{-4}$ (circles), $N = 80$, $\delta = 10^{-3}$ (squares), $N = 220$, $\delta = 10^{-3}$ (triangles down) and $\epsilon = 0.1, \delta = 10^{-2}$ (triangles up).

contrast, in the 'ferromagnetic' phase ($\epsilon N < 1$), it shows a periodic behavior around the initial conditions.

This behavior is quite typical in the study of dynamical systems, where the increase of a suitable perturbative parameter is related to the breaking of invariant tori and to the emergence of chaotic motion [20, 21].

It is also remarkable to study the fluctuations around the asymptotic behavior: in the undercritical case (figure 3(d)) fluctuations are much smaller than in the overcritical case (figure 3(c)), roughly ten times in this case, as can be seen by comparing the width of the probability distribution functions in figures 3(c) and (d).

The large fluctuations around the average values in order to fit a possible experimental situation suggest averaging over disorder, namely an ensemble of samples with different random configurations, initially magnetized along the z axis.

The results for the ensemble average $\langle M_z \rangle$ are shown in figure 4(a), where the different behaviors in the two 'phases' $\epsilon N < 1$ and $\epsilon N > 1$ are reflected in an average magnetization not decreasing or decreasing to zero. Indeed, the average magnetization in the undercritical regime reaches some equilibrium value different from zero after some initial decay, while in the overcritical regime it goes to zero in an algebraic way.

Ensemble fluctuations at the equilibrium are independent of ϵN in the paramagnetic phase while in the ferromagnetic one they are typically smaller and increasing as $\sqrt{\epsilon N}$.

They are presented in figure 4(b), where

$$\Delta M_z^{\mathrm{eq}} = \lim_{\tau \to \infty} \Delta M_z(\tau)$$

has been shown as a function of ϵN. On the vertical axis we renormalize the asymptotic values by $\sqrt{N}$ to take into account fluctuations due to variation of the number of spins N. Each series of points on the plot corresponds to an ensemble of magnetized needles, with the same concentration δ and number of spins N (paramagnetic ions) and different aspect ratio ϵ, or the same concentration and aspect ratio and different number of spins. It is quite remarkable that the critical value $\epsilon N \sim 1$ is well fitted by all different series, suggesting ϵN as a good scaling parameter for the macroscopic behavior.

Both the independence of the perturbation strength in the paramagnetic phase and the square root dependence on ϵN in the ferromagnetic phase can be understood on the basis of classical dynamical theory. Breaking invariant tori with a perturbation strength k corresponds to creating stochastic layers between invariant tori whose size is proportional to $\sqrt{k}$ [20, 21]. On the other side, when the system is completely chaotic, since the variable M_z is bounded, it can only occupy all the allowable stochastic region, and a further increasing of perturbation strength cannot modify this size.

Finally we point out that, around $\epsilon N = 1$, we can expect a transition from a ferromagnetic ground state to an antiferromagnetic ground state. Indeed for $\epsilon N \ll 1$ the system is close to a 1D arrangement of dipoles, so that the ground state will be ferromagnetic, as pointed out in section 2. On the other hand, for $\epsilon N \gg 1$ the system is close to a 3D arrangement of dipoles. In this case, for a simple cubic lattice, it can be shown [19] that the ground state is antiferromagnetic. Some numerical simulations we did confirm this conjecture, but work is still in progress and will be presented in a future publication.

4. Demagnetization time

As we have seen in section 3, the system dynamics can be described by the parameter, ϵN, characterizing two different dynamical phases, and describing how much one-dimensional a system is. In this section we will show that ϵN is also a good (and intensive) scaling parameter for the macroscopic properties of the quasi-1D system.

In order to prove numerically such an argument we need to find two physical observables that can describe the paramagnetic and the ferromagnetic phases and to study their dependence on the parameter ϵN. To this end, let us introduce, on the paramagnetic side, the demagnetization time $\tau_{1/2}$, defined as the time at which the average magnetization decays to one-half of its initial value:

$$\langle M_z(\tau_{1/2}) \rangle = (1/2)\langle M_z(0) \rangle.$$

In the same way, on the ferromagnetic side, we introduce the 'remnant magnetization' M_{r} as the magnetization left when $\tau \to \infty$:

$$M_{\mathrm{r}} = \lim_{\tau \to \infty} \langle M_z(\tau) \rangle.$$

Let us stress that both quantities are physically sound, in the sense that they are directly and easily measurable.
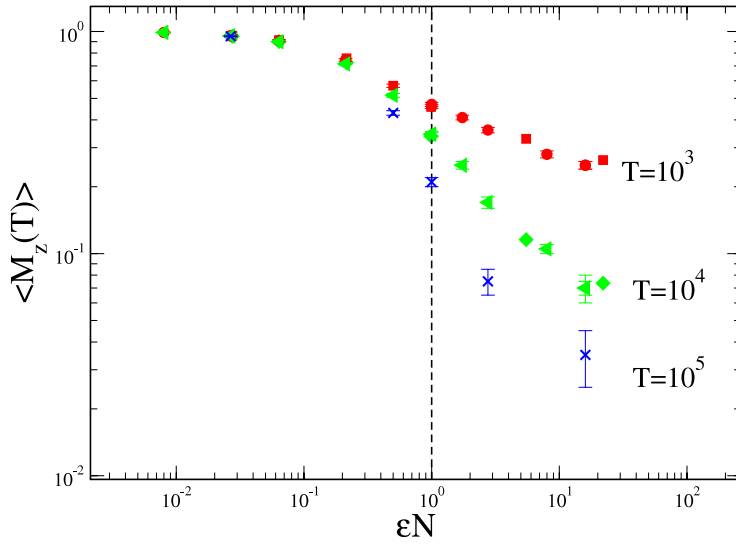
Figure 5. Average magnetization at time T as a function of ϵN. For the same ϵN we show the average magnetization after different simulation times, T. Data refer to the case $\delta = 10^{-3}$. Different numbers of dipoles are shown: $N = 220$ (circles for $T = 10^3$ and lozenges for $T = 10^4$) and $N = 80$ (squares for $T = 10^3$, left triangles for $T = 10^4$ and crosses for $T = 10^5$).

While it is clear that, even if both quantities can be defined only in their respective phases, they can give useful information when extended to the other phases. For instance, in the paramagnetic phase the average magnetization will depend strongly on the simulation time (τ), while in the ferromagnetic phase the demagnetization time is typically infinite[3]. The dependence of the average magnetization on the simulation time can give important information on the ferromagnetic–paramagnetic transition. Indeed we can expect a weak dependence of the average magnetization in the ferromagnetic region $\epsilon N < 1$, since the presence of quasi-constant motions freezes the magnetization while, in the paramagnetic phase, the average magnetization $\langle M_z(T) \rangle$ goes to zero as the simulation time grows. This fact is clearly shown in figure 5, where the average magnetization $\langle M_z(T) \rangle$ is plotted versus ϵN for different simulation times. As we can see from figure 5, as we increase the simulation time the average magnetization remains almost constant on the ferromagnetic side ($\epsilon N < 1$), while it goes to zero on the paramagnetic side ($\epsilon N > 1$), thus demonstrating a clear signature of the dimensional transition discussed above.

Since $\epsilon N = \delta R^3$, one can essentially consider different ways to approach the critical point $\epsilon N = \delta R^3 \simeq 1$, keeping fixed one of the four quantities ϵ, N, δ, R and correspondingly varying all the others. This is exactly what we did in figure 6, where we show, on the same plot, the remnant magnetization M_r (open symbols and vertical axis to the left) and the inverse demagnetization time $(\tau_{1/2}\delta)$, rescaled by the concentration δ (vertical axis to the right, full symbols) both as a function of the parameter ϵN. Reserving later on the discussion about the time-rescaling with δ, let us observe two relevant features. The first is the presence of a change of curvature of both curves on approaching the critical border

---

[3] In this case we underestimate its value, putting as a magnetization time the maximum dimensionless simulation time, which is 10^4.
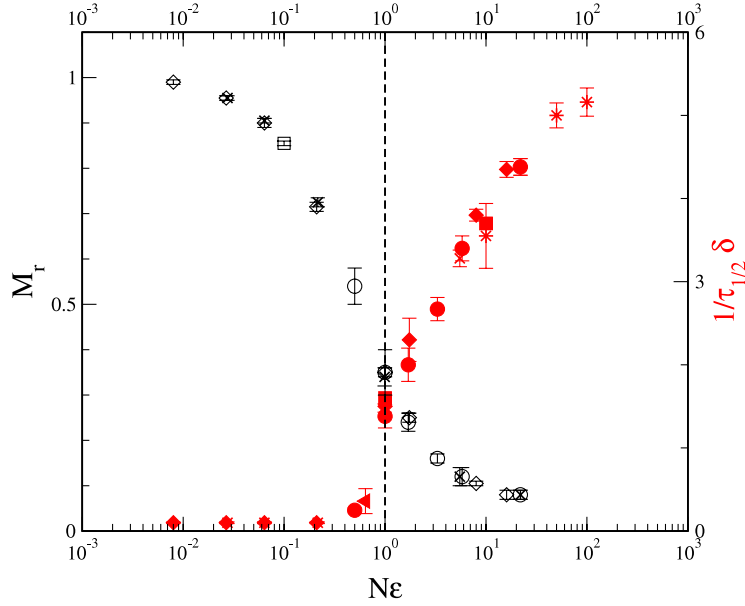
Figure 6. Inverse demagnetization time $\tau_{1/2}$ rescaled by the concentration δ versus the parameter ϵN: full symbols should be read on the right vertical axis. Remnant magnetization M_r versus the parameter ϵN: open symbols read on the left vertical axis. Circles ($\epsilon = 0.1, \delta = 10^{-3}$), lozenges ($N = 80, \delta = 0.01$), crosses ($N = 220, \delta = 10^{-3}$), squares ($N = 100, R = 4$), asterisks ($N = 500, R = 20$) and left triangles ($\epsilon = 0.01, \delta = 0.01$). Initially we choose $S_i^z(0) = 1$, $i = 1, \ldots, N$. In this figure an ensemble of 100 different configurations has been considered. Each member of the ensemble has been integrated for 10^4 dimensionless time units.

$\epsilon N = \delta R^3 \simeq 1$. The second is the scaling of all points in the two curves (one for $\tau_{1/2}\delta$ and the other for the remnant magnetization M_r).

As for the rescaling of the time, let us observe that, due to the particular quasi-1D geometry, and to the low concentration $\delta \ll 1$, closest dipoles give the major contribution to the energy. For instance, the configuration with all spins aligned along the z axis will have an energy

$$E' \propto \sum_{\langle i,j \rangle} \frac{1}{|r_{ij}|^3}, \tag{11}$$

where the sum is taken over N couples $\langle i, j \rangle$ of neighbor dipoles. In other words, $E' \sim N/d^3 \sim N\delta$, where d is the average distance between two dipoles.

On the other hand, the Landau–Lifshitz–Gilbert equations of motion are invariant under a simultaneous scaling of time and energy $\tau' = \tau/\delta$ and $E' = E\delta$ so that we will expect $\tau \propto 1/\delta$. This simple relation has been verified considering a system with the same aspect ratio ϵ and the same number of particles N (so as to have the same value of ϵN) and changing the concentration δ over three orders of magnitude. Results are presented in figure 7(a), where $\tau_{1/2}$ has been shown versus δ. To guide the eye a dashed line indicating the inverse proportionality has been superimposed. As one can see, looking
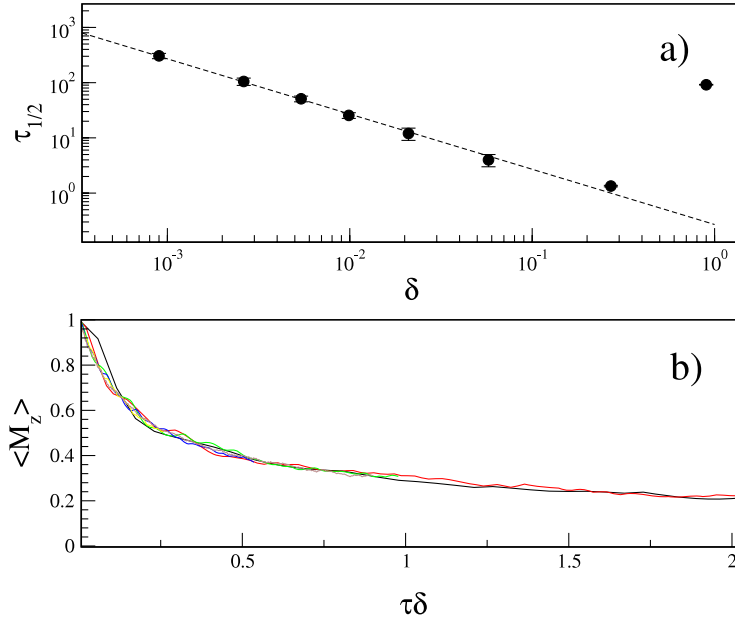
Figure 7. (a) Dependence of the average demagnetization time $\tau_{1/2}$ as a function of concentration δ, for systems with $\epsilon = 0.1$ and $N = 72$. The average has been taken over an ensemble of 100 different samples. Initially all samples have all spins aligned along the z axis: $S_i^z(0) = 1$, $i = 1, \ldots, N$. Dashed line represents $\tau_{1/2} \propto 1/\delta$. (b) Average magnetization $\langle M_z(\tau) \rangle$ as a function of the rescaled time $\tau\delta$ for different concentrations δ and fixed $\epsilon = 0.1$, and $N = 72$ as in (a).

at the last point to the right-hand side of figure 7(a), this relation does not hold true for concentrations $\delta \simeq 1$, where the nearest-neighbor approximation (11) fails.

The 'scale invariance' is even more evident if the average magnetization is considered as a function of the rescaled time $\tau\delta$, shown in figure 7(b), for the same cases belonging to the straight line shown in figure 7(a).

At last, we investigate the system behavior on approaching the large N limit. First of all let us observe that the scaling variable $\epsilon N = RN/L$ is well defined in the large N limit $N, L \to \infty$, $N/L = \text{const}$ and R fixed[4].

In order to do that we take into account different systems with fixed concentration δ and radius R and increasing length L and number of particles N: both in the ferromagnetic phase $\epsilon N < 1$ (figure 8(a)) and in the paramagnetic one $\epsilon N > 1$ (figure 8(b)), the average magnetization is independent of the number of particles N.

5. Conclusions

In this paper the microcanonical dynamics of a system of random dipoles, interacting with a pure dipole–dipole interaction, has been considered. We have shown that a dimensional 'phase' transition, correspondent to a transition from the regular (ferromagnetic) to the stochastic (paramagnetic) regime occurs, in the microcanonical ensemble, for low concentration δ. Such a transition is characterized from the dynamical point of view by a

---

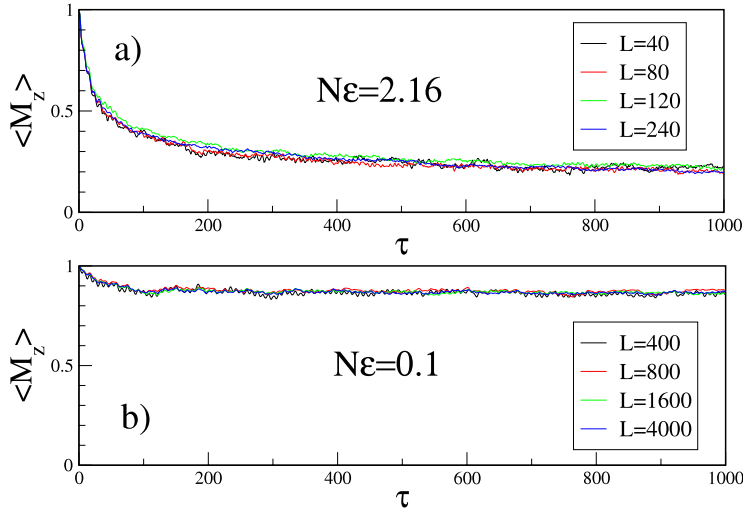[4] We thank the referee for this remark.

Figure 8. Average magnetization $\langle M_z \rangle$ versus the dimensionless time τ, for different sample lengths L, as indicated in the legend, and different numbers of spins N, at fixed density ($N/L = 0.36$) for the paramagnetic phase $N\epsilon = 2.16$ (a), and for the ferromagnetic one $\epsilon N = 0.1$ (b). In (a) $R = 6$, $\delta = 0.01$, while in (b) $R = 4$ and $\delta = 0.001\,5625$. Initially we choose $S_i^z(0) = 1$, $i = 1, \ldots, N$. An ensemble of 100 different configurations has been considered.

different behavior of the fluctuations of the average magnetization, and from the physical point of view, respectively, by a zero remnant magnetization, $M_r = \lim_{\tau \to \infty} \langle M_z(\tau) \rangle$, and finite decay rates, $\propto 1/\tau_{1/2}\delta$ (paramagnetic phase) or zero decay rates and finite remnant magnetization (ferromagnetic phase). We showed that this dimensional transition occurs when the intensive parameter $\epsilon N = 1$, where ϵ is the aspect ratio and N is the number of dipoles. For instance, in an experimental situation if we have a non-magnetic substrate with $R = 1.6$ nm and $L = 1.6$ μm, with a lattice size of ≈ 4 Å, we expect a dimensional transition for $\delta = 0.15\%$. We also conjectured that, in correspondence to this transition, the ground state changes from ferromagnetic to antiferromagnetic.

In the future we would like to investigate dilute dipole systems in the canonical ensemble, that is letting the system be in contact with a thermal bath. Our analysis in the microcanonical ensemble indicated that the behavior of very dilute dipoles in a needle geometry is very similar to a 1D array of dipoles. In the 1D case dipole interaction induces a ferromagnetic ground state and, due to its anisotropy, to a breaking of ergodicity [3]. As shown in [23], the ergodicity breaking threshold can induce very large demagnetization times, thus producing ferromagnetic behavior in finite samples. Thus, even if one would expect that invariant tori will be destroyed under a suitable thermal perturbation, the question of the demagnetization times in the presence of temperature and on the relevance of the ergodicity breaking is still open.

The ergodicity breaking found in [3] considers the total magnetization as an order parameter. On the other hand, different order parameters can be defined in dipole systems, depending on the ground state configuration, for instance an antiferromagnetic order parameter or a spin glass order parameter. Therefore, it would be interesting to investigate the existence of an ergodicity breaking energy threshold with respect to different order parameters.

In conclusion dipole–dipole interacting spin systems offer a realistic playground to analyze many properties of magnetic systems which challenge our comprehension.

Acknowledgments

References

[1] Coey J M, Venkatesan M and Fitzgerald C B, 2005 *Nat. Mater.* **4** 173
    Sangaletti L, Mozzati M C, Drera G, Galinetto P, Azzoni C B, Speghini A and Bettinelli M, 2008 *Phys. Rev.* B **78** 075210
[2] Palmer R G, 1982 *Adv. Phys.* **31** 669
[3] Borgonovi F, Celardo G L, Maianti M and Pedersoli E, 2004 *J. Stat. Phys.* **116** 516
[4] Mukamel D, Ruffo S and Schreiber N, 2005 *Phys. Rev. Lett.* **95** 240604
    Bouchet F, Dauxois T, Mukamel D and Ruffo S, 2008 *Phys. Rev.* E **77** 011125
    Campa A, Khomeriki R, Mukamel D and Ruffo S, 2007 *Phys. Rev.* B **76** 064415
    Campa A, Dauxois T and Ruffo S, 2009 *Phys. Rep.* **480** 57
[5] Van Enter A C D and Van Hemmen J L, 1984 *Phys. Rev.* A **29** 355
[6] Dauxois T, Ruffo S, Arimondo E and Wilkens M (ed), 2002 *Springer Lecture Notes in Physics* vol 602 (Berlin: Springer)
[7] Borgonovi F, Celardo G L, Musesti A, Trasarti-Battistoni R and Vachal P, 2006 *Phys. Rev.* E **73** 026116
[8] Luttinger J M and Tisza L, 1946 *Phys. Rev.* **70** 954
    Luttinger J M and Tisza L, 1947 *Phys. Rev.* **72** 257
[9] Yu C C, 1992 *Phys. Rev. Lett.* **69** 2787
[10] Jensen S J K and Kjaer K, 1989 *J. Phys.: Condens. Matter* **1** 2361
[11] Xu H-J, Bergersen B, Niedermayer F and Rácz Z, 1991 *J. Phys.: Condens. Matter* **3** 4999
[12] Snider J and Yu C C, 2005 *Phys. Rev.* B **72** 214203
[13] Tam K-M and Gingras M J, 2009 *Phys. Rev. Lett.* **103** 087202
[14] Dauxois T, Ruffo S and Cugliandolo L F, *Long-range interacting systems*, 2008 *Lecture Notes of the Les Houches Summer School* vol 90 (Oxford: Oxford University Press)
[15] Vugmeister B E and Glinchuk M D, 1990 *Rev. Mod. Phys.* **62** 993
[16] Zhang H and Widom M, 1995 *Phys. Rev.* B **51** 8951
[17] Stephen M J and Aharony A, 1981 *J. Phys. C: Solid State Phys.* **14** 1665
[18] Ayton G, Gingras M J P and Patey G N, 1997 *Phys. Rev.* E **56** 562
[19] Sauer J A, 1940 *Phys. Rev.* **57** 140
[20] Chirikov B V, 1979 *Phys. Rep.* **52** 263
[21] Lichtenberg A J and Lieberman M A, 1983 *Regular and Stochastic Motion* (*Applied Math. Series* vol 38) (Berlin: Springer)
[22] Celardo G, Barré J, Borgonovi F and Ruffo S, 2006 *Phys. Rev.* E **73** 011108
[23] Borgonovi F, Celardo G L, Goncalves B and Spadafora L, 2008 *Phys. Rev.* E **77** 061119